Preprints of the 22nd IFAC World Congress
Yokohama, Japan, July 9-14, 2023

Point-mass Filter with Functional Decomposition of Transient Density and Two-level Convolution ⋆

Ondřej Straka * **Jindřich Duník** * **Petr Tichavský** **

* *Department of Cybernetics, European Centre of Excellence NTIS, Faculty of Applied Sciences, University of West Bohemia, Pilsen, Czech Republic (e-mail: {straka30,dunikj}@ kky.zcu.cz).*
** *The Czech Academy of Sciences, Institute of Information Theory and Automation, Prague, Czech Republic. (e-mail: tichavsk@utia.cas.cz).*

Abstract: The paper deals with Bayesian state estimation using the point-mass filter with a particular focus on the prediction step involving the convolution of two grids of points. To reduce the computational costs of the step, a functional decomposition-based convolution was proposed by Tichavský et al. (2022), which approximates the transient probability density function over an approximation region. This paper addresses the problem of having spacious grids of points due to state uncertainty while the approximation region is kept small to preserve low computational complexity. A two-level convolution is proposed based on splitting the grids into subgrids and processing the convolution in the upper level for the subgrids and in the lower level for their points. An example demonstrates the proposed technique efficiency.

Keywords: Bayesian methods; state estimation; point-mass filter; transient density; functional decomposition

1. INTRODUCTION

The state estimation of nonlinear discrete-time stochastic dynamic systems from noisy measurements is vital for many domains, such as tracking and navigation, optimal and adaptive control, signal processing, and fault detection.

A solution to the state estimation problem formulated as an inference of the probability density functions (PDFs) of the state conditioned by the available measurements is given by the Bayesian recursive relations (BRRs). The BRRs are intractable in general, with the exception of a few special cases, such as linear models with Gaussian distributed noises. Hence, for nonlinear models with non-Gaussian uncertainties, the BRR solution is typically subject to approximations. Gaussian approximations of the conditional densities lead to popular computationally cheap solutions (Arasaratnam and Haykin, 2009). However, for highly nonlinear models they offer limited estimate accuracy (Särkkä, 2013). High-quality estimates are provided in these cases by methods representing the posterior PDF of the state by particle-based approximations (Doucet et al., 2001), Gaussian mixture approximations (Sorenson and Alspach, 1971), or point-mass approximations (Šimandl et al., 2002; Duník et al., 2019). High quality, however, comes with substantial computational demands.

This paper focuses on the point-mass filter (PMF) (Šimandl et al., 2006; Matoušek et al., 2019) that calculates the point-mass approximations of the conditional PDFs. The PMF uses *deterministic* grid-based numerical integration rules and computes the conditional PDFs only at the grid points. A suitable specification of the number of grid points is critical as it affects the estimate accuracy and computational complexity. The computational bottleneck of the standard filter implementation, which limits the number of the grid points from above, is the predictive step. This step involves an evaluation of a convolution called the Chapman-Kolmogorov equation, where the grids for conditional PDFs at two consecutive time instants are combined through the transient PDF. The convolution complexity thus grows quadratically with the number of the grid points N.

Many techniques for PMF computational complexity reduction were proposed, often at the cost of extra approximations, the need for user-defined parameters, or only for particular models. The techniques are based on:

- *Rao-Blackwellization:* The techniques assume the conditionally linear models with Gaussian noises, where the expensive PMF estimates the nonlinearly modeled part of the state whereas the remaining linearly modeled part is estimated by computationally cheap Kalman filters (Duník et al., 2019; Lim and Park, 2019).
- *Separable prediction:* These techniques assume a particular model and Gaussian noise and evaluate the transient PDF off-line. They do not use the convolution theorem, and the complexity depends on the state noise variance. In the worst-case scenario, it is still $\mathcal{O}(N^2)$ (Bergman, 1999).
- *Copula prediction:* Instead of propagating the conditional PDF, these techniques propagate the marginal PDFs and a copula (Nelsen, 2006), capturing the correlation. An optimal copula cannot generally be found; thus, its selection is a designer decision leading to an extra approximation error (Duník et al., 2022).

The PMF grid can also be designed using adaptive or sparse layouts (Kalender and Schottl, 2013). This leads to a reduction of the total number of grid point N , the order of the complexity is still $\mathcal{O}\left(N^2\right)$.

⋆ The work was supported by the Czech Science Foundation under grant 22-11101S.

Tichavský et al. (2022) proposed an entirely different approach based on *functional tensor decomposition* (FTD) to tackle to issue. The decomposition is based on the non-negative matrix factorization [1] (NNMF) and symmetric NNMF (Huang et al., 2014). The technique decomposes the transient PDF into a sum of R products of functions of current and future states, where R is the FTD rank. The complexity induced by the FTD-based technique is $\mathcal{O}((2N+1)R)$.

The FTD-based technique approximates the transient PDF on a selected region, inducing approximation error that can be adjusted by the rank R. Besides the error-related adjustment, the rank depends on the size of the region. When preserving a fixed error, the rank proliferates (Tichavský et al., 2022) with increasing state dimension. To keep low complexity, the rank should be kept as small as possible. While ensuring fixed error, the rank can be decreased by reducing the size of the approximation region. On the other hand, the proposed FTD-based technique requires the grids representing the conditional PDF of the state to fit into the region, which hampers the size reduction. The paper aims to address these conflicting requirements by introducing a two-level convolution that facilitates using small approximation regions with spacious grids.

The paper is structured as follows: Section 2 briefly introduces Bayesian inference for state estimation of nonlinear non-Gaussian models by the PMF and describes the FTD of the transient PDF. The problem related to the approximation region is analyzed, and the two-level convolution is proposed in Section 3. A numerical illustration of the two-level convolution is presented in Section 4, and Section 5 gives concluding remarks.

2. STATE ESTIMATION BY POINT-MASS METHOD

2.1 State Estimation

Consider the following discrete-time state-space model of a nonlinear stochastic dynamic system with additive noises

$$\mathbf{x}_{k+1} = \mathbf{f}_k(\mathbf{x}_k, \mathbf{u}_k) + \mathbf{w}_k, \qquad k = 0, 1, 2, \dots, T, \tag{1}$$

$$\mathbf{z}_k = \mathbf{h}_k(\mathbf{x}_k) + \mathbf{v}_k, \qquad k = 0, 1, 2, \dots, T, \tag{2}$$

where $\mathbf{x}_k \in \mathbb{R}^{n_x}$, $\mathbf{u}_k \in \mathbb{R}^{n_u}$, and $\mathbf{z}_k \in \mathbb{R}^{n_z}$ represent the *unknown* state of the system, *known* input, and measurement at time instant k, respectively. The state and measurement functions $\mathbf{f}_k : \mathbb{R}^{n_x} \times \mathbb{R}^{n_u} \to \mathbb{R}^{n_x}$ and $\mathbf{h}_k : \mathbb{R}^{n_x} \to \mathbb{R}^{n_z}$ are *known* vector transformations. The state and measurement noises $\mathbf{w}_k \in \mathbb{R}^{n_x}$ and $\mathbf{v}_k \in \mathbb{R}^{n_z}$ are described by *known* PDFs, i.e., the state noise PDF $p(\mathbf{w}_k)$ and the measurement noise PDF $p(\mathbf{v}_k)$. The initial state is characterized by *known* PDF $p(\mathbf{x}_0)$. The noises $\mathbf{w}_k$, $\mathbf{v}_k$, and the initial condition $\mathbf{x}_0$ are independent. The model (1) and (2) can equivalently be described by the state transient PDF $p(\mathbf{x}_{k+1}|\mathbf{x}_k) = p_{\mathbf{w}_k}\big(\mathbf{x}_{k+1} - \mathbf{f}_k(\mathbf{x}_k, \mathbf{u}_k)\big)$ and the measurement PDF $p(\mathbf{z}_k|\mathbf{x}_k) = p_{\mathbf{v}_k}\big(\mathbf{z}_k - \mathbf{h}_k(\mathbf{x}_k)\big)$, respectively.

The goal of the state estimation is to infer the posterior PDF $p(\mathbf{x}_k|\mathbf{z}^k), \forall k$ conditioned on all measurements up to the time instant k, which are denoted as $\mathbf{z}^k := [\mathbf{z}_0^\top, \mathbf{z}_1^\top, \dots, \mathbf{z}_k^\top]^\top$. The BRRs give general solution to the state estimation in the form of conditional PDFs [2] (Särkkä, 2013)

$$p(\mathbf{x}_k|\mathbf{z}^k) = \frac{p(\mathbf{x}_k|\mathbf{z}^{k-1})p(\mathbf{z}_k|\mathbf{x}_k)}{p(\mathbf{z}_k|\mathbf{z}^{k-1})}, \tag{3}$$

$$p(\mathbf{x}_{k+1}|\mathbf{z}^k) = \int p(\mathbf{x}_{k+1}|\mathbf{x}_k)p(\mathbf{x}_k|\mathbf{z}^k)d\mathbf{x}_k, \tag{4}$$

where $p(\mathbf{x}_{k+1}|\mathbf{z}^k)$ is the one-step predictive PDF computed by the Chapman-Kolmogorov equation (CKE) (4) and $p(\mathbf{x}_k|\mathbf{z}^k)$ is the filtering PDF computed by the Bayes rule (3). The PDF $p(\mathbf{z}_k|\mathbf{z}^{k-1}) = \int p(\mathbf{x}_k|\mathbf{z}^{k-1})p(\mathbf{z}_k|\mathbf{x}_k)d\mathbf{x}_k$ is the one-step predictive PDF of the measurement. The recursion (3), (4) starts from $p(\mathbf{x}_0|\mathbf{z}^{-1}) = p(\mathbf{x}_0)$.

2.2 Point-mass Method

The PMF approximates the conditional PDF $p(\mathbf{x}_k|\mathbf{z}^m)$, $(m \in \{k-1, k\})$ by a weighted set of N grid points $\Xi_k = \{\boldsymbol{\xi}_k^{(i)}\}_{i=1}^N$ as

$$p(\mathbf{x}_k|\mathbf{z}^m) \approx \sum_{i=1}^{N} \omega_{k|m}^{(i)} S\{\mathbf{x}_k; \boldsymbol{\xi}_k^{(i)}, \boldsymbol{\Delta}_k\}, \tag{5}$$

with $S\{\mathbf{x}_k; \boldsymbol{\xi}_k^{(i)}, \Delta_k\}$ being the *selection* function defined as

$$S\{\mathbf{x}_k; \boldsymbol{\xi}_k^{(i)}, \Delta_k\} = \begin{cases} 1, & \text{if } \left|[\mathbf{x}_k]_j - [\boldsymbol{\xi}_k^{(i)}]_j\right| \le \frac{[\boldsymbol{\Delta}_k]_j}{2},\ j = 1, \dots, n \\ 0, & \text{otherwise,} \end{cases} \tag{6}$$

where the notation $[\cdot]_j$ stands for the j-th element of the involved vector. Thus, the selection function is uniform over the $\boldsymbol{\Delta}_k$-neighborhood of the grid point $\boldsymbol{\xi}_k^{(i)} \in \mathbb{R}^{n_x}$. The corresponding weight $\omega_{k|m}^{(i)} \in \mathbb{R}_{0+}$ is then given as

$$\omega_{k|m}^{(i)} = c_{k|m}\tilde{\omega}_{k|m}^{(i)}, \tag{7}$$

where $\tilde{\omega}_{k|m}^{(i)} = p_{\mathbf{x}_k|\mathbf{z}^m}(\boldsymbol{\xi}_k^{(i)}|\mathbf{z}^m)$ is the conditional PDF $p(\mathbf{x}_k|\mathbf{z}^m)$ evaluated at the i-th grid point $\boldsymbol{\xi}_k^{(i)}$, and $c_{k|m} = (\delta_k \sum_{i=1}^N \tilde{\omega}_{k|m}^{(i)})^{-1}$ is a normalization constant, $\delta_k := \prod_i [\boldsymbol{\Delta}_k]_i$. The basic algorithm of the PMF can be summarized as (Šimandl et al., 2006):

Algorithm 1: Point-Mass Filter

(1) *Initialization*: Set $k = 0$, construct the initial grid of points Ξ_k, and define the initial point-mass PDF $\hat{p}(\mathbf{x}_k|\mathbf{z}^{k-1})$ of the form (5) approximating the initial PDF.

(2) *Meas. update*: Compute the filtering point-mass PDF $\hat{p}(\mathbf{x}_k|\mathbf{z}^k)$ of the form (5) where the PDF value at i-th grid point is

$$\omega_{k|k}^{(i)} = \frac{p(\mathbf{z}_k|x_k=\xi_k^{(i)})\,\omega_{k|k-1}^{(i)}}{\sum_{i=1}^N p(\mathbf{z}_k|x_k=\xi_k^{(i)})\,\omega_{k|k-1}^{(i)}\delta_k}. \tag{8}$$

(3) *Grid construction:* Construct the new [3] grid Ξ_{k+1}.

(4) *Time update*: Compute the predictive point-mass PDF of the form (5) at the new grid of points, $\omega_{k+1|k}^{(j)} = c_{k+1}^{-1}\tilde{\omega}_{k+1|k}^{(j)}$, where

$$\tilde{\omega}_{k+1|k}^{(j)} = \sum_{i=1}^{N} p_{x_{k+1}|x_k}(\xi_{k+1}^{(j)}|x_k = \xi_k^{(i)})\omega_{k|k}^{(i)}\delta_k, \tag{9}$$

and c_{k+1} is a normalization given by $c_{k+1} = \sum_{j=1}^N \tilde{\omega}_{k+1|k}^{(j)}$.

(5) Set $k = k+1$ and go to Step 2.

[1] The NNMF originally known as non-negative rank factorization or positive matrix factorization has been subject to intensive research for more than three decades (Chen, 1984), (Paatero and Tapper, 1994).

[2] Considering the model (1), (2), the BRRs (3), (4) should also be conditioned on the *available* sequence of the inputs $\mathbf{u}_k$. However, for the sake of convenience, the input signal is assumed to be implicitly part of the condition and it is not explicitly stated, i.e., $p(\mathbf{x}_{k+1}|\mathbf{x}_k) = p(\mathbf{x}_{k+1}|\mathbf{x}_k; \mathbf{u}_k)$, $p(\mathbf{x}_k|\mathbf{z}^k) = p(\mathbf{x}_k|\mathbf{z}^k; \mathbf{u}^{k-1})$, and $p(\mathbf{x}_{k+1}|\mathbf{z}^k) = p(\mathbf{x}_{k+1}|\mathbf{z}^k; \mathbf{u}^k)$.

[3] Usually, the number of grid points N is kept constant $\forall k$ to ensure constant (and predictable) computational complexity of the PMF.

Standard PMF computes the weights $\omega^{(j)}_{k+1|k}$ by evaluating the transient PDF $p(\mathbf{x}_{k+1}|\mathbf{x}_k)$ for all combinations of the grid points Ξ_{k+1} and Ξ_k. This gives N^2 evaluations leading to high computational complexity, particularly for large n_x as N is chosen as $N = (N_a)^{n_x}$, where N_a is the number of grid points per an axis. Such a procedure will be called full convolution (FC). To address this issue, Šimandl et al. (2002) proposed a technique called thrifty convolution (TC) based on calculating $\tilde{\omega}^{j}_{k+1|k}$ as

$$\tilde{\omega}^{(j)}_{k+1|k} = \sum_{\xi^i_k \in \Lambda_k} p_{x_{k+1}|x_k}(\xi^{(j)}_{k+1}|x_k = \xi^{(i)}_k)\omega^{(i)}_{k|k}\delta_k, \qquad (10)$$

where $\Lambda_k \subseteq \Xi_k$ is a subset of Ξ_k such that its elements lie within a neighborhood of $\xi^{(j)}_{k+1}$.

2.3 Functional Decomposition of Transient Density

Using the FTD of the transient PDF (Tichavský et al., 2022) is another approach to address the issue. The approach approximates the transient PDF by a functional decomposition [4] as

$$p(\mathbf{x}_{k+1}|\mathbf{x}_k) \approx \hat{p}(\mathbf{x}_{k+1}|\mathbf{x}_k) = \sum_{r=1}^{R} \mathcal{F}^r_1(\mathbf{x}_{k+1})\mathcal{F}^r_2(\mathbf{x}_k), \qquad (11)$$

where $\mathcal{F}^r_1(\cdot), \mathcal{F}^r_2(\cdot)$, $r = 1, \dots, R$ are suitable (non-negative) functions, designed in advance, and R is the order of the approximation called a *rank*.

Given (11), the CKE (4) can be written as

$$p(\mathbf{x}_{k+1}|\mathbf{z}^k) \approx \sum_{r=1}^{R} \mathcal{F}^r_1(\mathbf{x}_{k+1}) \int \mathcal{F}^r_2(\mathbf{x}_k)p(\mathbf{x}_k|\mathbf{z}^k)d\mathbf{x}_k. \qquad (12)$$

The simplification of using (12) in (9) is that R integrals in (4) can be computed at the grid points Ξ_k only, without the need to consider the combination of all grid points Ξ_{k+1} for $\mathbf{x}_{k+1}$ and all grid points Ξ_k for $\mathbf{x}_k$.

For the point-mass approximation (5) of $p(\mathbf{x}_k|\mathbf{z}^k)$ the integral in (12) is [5]

$$\int \mathcal{F}^r_2(\mathbf{x}_k)p(\mathbf{x}_k|\mathbf{z}^k)d\mathbf{x}_k \approx \sum_{i=1}^{N} \mathcal{F}^r_2(\xi^{(i)}_k)\omega^{(i)}_{k|k}\delta_k =: \mathcal{I}^r_k. \qquad (13)$$

The values of the predictive PDF (12) are then given as

$$\tilde{\omega}^{(j)}_{k+1|k} = \sum_{r=1}^{R} \mathcal{F}^r_1(\xi^{(j)}_{k+1}) \sum_{i=1}^{N} \mathcal{F}^r_2(\xi^{(i)}_k)\omega^{(i)}_{k|k}\delta_k = \sum_{r=1}^{R} \mathcal{F}^r_1(\xi^{(j)}_{k+1})\mathcal{I}^r_k. \qquad (14)$$

3. TWO-LEVEL CONVOLUTION

3.1 Analysis of Functional Decomposition

The model (1) with additive noise [6] is advantageous for the FTD as the transient PDF depends only on the difference of $\mathbf{x}_{k+1} - \mathbf{f}_k(\mathbf{x}_k, \mathbf{u}_k)$ as

[4] Relation (11) can be seen as a particular case of the functional tensor-based decomposition (Gorodetsky et al., 2018) where the functions $\mathcal{F}^r_1$ and $\mathcal{F}^r_2$ are not decomposed further to functions of single elements of $\mathbf{x}_{k+1}$ and $\mathbf{x}_k$.

[5] For convenience, the constant number N of grid points of Ξ_{k+1} and Ξ_k is considered.

[6] Note that the FTD can be used in principle even for models with non-additive noises. It may however require construction of the decomposition over a larger area, which is connected with higher rank and higher computational costs.

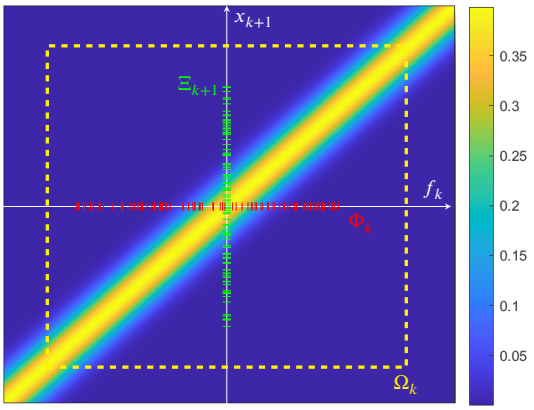

Fig. 1. Illustration of the Gaussian transient PDF $p(x_{k+1}|f_k) = p_{w_k}(x_{k+1} - f_k)$ (colored background)), the approximation region Ω, and the grids Ξ_{k+1} and Φ_k for x_{k+1} and f_k, respectively.

$$p(\mathbf{x}_{k+1}|\mathbf{x}_k) = p_{\mathbf{w}_k}(\mathbf{x}_{k+1} - \mathbf{f}_k), \qquad (15)$$

where the notation $\mathbf{f}_k := \mathbf{f}_k(\mathbf{x}_k, \mathbf{u}_k)$ is introduced for convenience. Expressing the transient PDF (15) in terms of $\mathbf{x}_{k+1}$ and $\mathbf{f}_k$ is substantially simpler [7] than expressing the PDF $p(\mathbf{x}_{k+1}|\mathbf{x}_k) = p_{\mathbf{w}_k}(\mathbf{x}_{k+1} - \mathbf{f}_k(\mathbf{x}_k, \mathbf{u}_k))$ in terms of $\mathbf{x}_{k+1}$ and $\mathbf{x}_k$, especially for highly nonlinear $\mathbf{f}_k(\cdot,\cdot)$. Thus, the approximate transient PDF will be further expressed in terms of $\mathbf{x}_{k+1}$ and $\mathbf{f}_k$ as follows

$$\hat{p}(\mathbf{x}_{k+1}|\mathbf{x}_k) = \hat{p}(\mathbf{x}_{k+1}|\mathbf{f}_k) = \sum_{r=1}^{R} \mathcal{F}^r_1(\mathbf{x}_{k+1})\mathcal{F}^r_2(\mathbf{f}_k), \qquad (16)$$

The grid Ξ_k for $\mathbf{x}_k$ can then be transformed to a grid $\Phi_k := \{\boldsymbol{\phi}^{(i)}_k\}_{i=1}^N$ for $\mathbf{f}_k$, where $\boldsymbol{\phi}^{(i)}_k = \mathbf{f}_k(\xi^{(i)}_k, \mathbf{u}_k)$. Remark that the grid Φ_k serves as a foundation for designing the grid Ξ_{k+1}. The approximation (16) is calculated in an approximation region $\Omega_k \subset \mathbb{R}^{n_x}$ for $\mathbf{x}_{k+1}$ and $\mathbf{f}_k$. For $n_x = 1$ and standard Gaussian PDF $p(w_k)$, the transient PDF $p(x_{k+1}|x_k) = p_{w_k}(x_{k+1} - f_k)$, the grids Ξ_{k+1}, Φ_k and the approximation region Ω_k are illustrated in Figure 1.

The approximation region should cover the space, where the PDF $p_{\mathbf{w}_k}$ is non-negligible. Its size affects the rank R of the approximation. Enlarging the region while keeping the approximation error fixed leads to an increase in the rank, which should be avoided, especially for higher dimensions n_x. When the PDF $p_{\mathbf{w}_k}$ is time-invariant, the region can be *fixed*, $\Omega_k = \Omega$, $\forall k$. Hence, if either gridpoints of Ξ_{k+1} or gridpoints of Φ_k do not fit into the fixed region Ω, they can be conveniently shifted by some $\boldsymbol{\zeta} \in \mathbb{R}^{n_x}$ to the region as $p_{\mathbf{w}_k}(\xi^{(j)}_{k+1} - \boldsymbol{\phi}^{(i)}_k) = p_{\mathbf{w}_k}\left((\xi^{(j)}_{k+1} - \boldsymbol{\zeta}) - (\boldsymbol{\phi}^{(i)}_k - \boldsymbol{\zeta})\right)$. Shifting each pair of the gridpoints $\xi^{(j)}_{k+1}$ and $\boldsymbol{\phi}^{(i)}_k$, $i, j = 1, \dots, N$ individually by some $\boldsymbol{\zeta}^{i,j}$ (i.e., each pair $\xi^{(j)}_{k+1}$ and $\boldsymbol{\phi}^{(i)}_k$ takes a different shift $\boldsymbol{\zeta}^{i,j}$) is highly inefficient as there are N^2 different pairs, and the number of shifts would also be N^2. The aim of the FTD to avoid such combinations when calculating the predictive PDF values (9). Hence, in (Tichavský et al., 2022), the entire grids Ξ_{k+1} and Φ_k are shifted by a single value $\boldsymbol{\zeta}$ calculated as a mean of all points in both grids

[7] Note that $\mathbf{f}_k$ is a random variable obtained by transforming the random variable $\mathbf{x}_k$ through $\mathbf{f}_k(\cdot, \mathbf{u}_k)$.

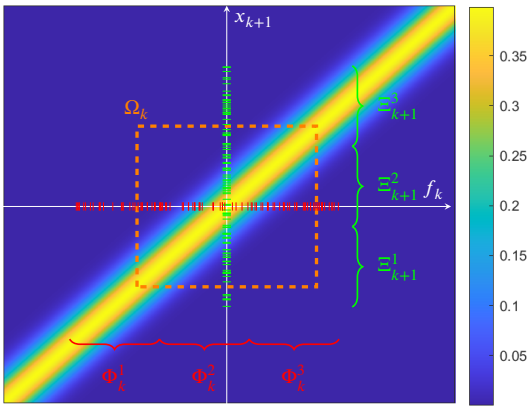

Fig. 2. Illustration of the Gaussian transient PDF $p(x_{k+1}|f_k) = p_{w_k}(x_{k+1} - f_k)$ (colored background)), the approximation region Ω, and the grids Ξ_{k+1} and Φ_k for x_{k+1} and f_k, respectively, each split into three subgrids.

$$\zeta = \frac{1}{2N}\left(\sum_{i=1}^{N} \boldsymbol{\phi}_k^{(i)} + \sum_{j=1}^{N} \boldsymbol{\xi}_{k+1}^{(i)}\right). \tag{17}$$

Using this value to shift both grids places the centers of the grids as close as possible to the origin where the center of approximation region Ω is placed.

3.2 Idea of Two-level Convolution

This paper addresses the situation when the grids Ξ_{k+1} and Φ_k after the shifting cover space larger than Ω and enlarging Ω is to be avoided. For convenience, the time index subscripts will be dropped in the following part, e.g., $\Xi := \Xi_{k+1}$. The idea is to split the grids Ξ and Φ into subgrids and treat each subgrid individually. In particular, when $n_x = 1$, the grid Ξ is split into N_Ξ subgrids $\{\Xi^j\}_{j=1}^{N_\Xi}$ such that

$$\boldsymbol{\xi}' < \boldsymbol{\xi}'', \ \forall\, \boldsymbol{\xi}' \in \Xi^i, \forall\, \boldsymbol{\xi}'' \in \Xi^j, \ i < j$$

and by analogy, the grid Φ is split into N_Φ subgrids $\{\Phi^j\}_{j=1}^{N_\Phi}$. Each subgrid should fit into the approximation region Ω. The splitting is illustrated in Figure 2 for $n_x = 1$. Note that the splitting for $n_x > 1$ will be described later.

The non-normalized predictive PDF value (14) for a point $\boldsymbol{\xi} \in \Xi^j$ can then be written as

$$\begin{aligned}\tilde{\omega}_{k+1|k}(\boldsymbol{\xi}) &= \sum_{r=1}^{R} \mathcal{F}_1^r(\boldsymbol{\xi}) \sum_{i=1}^{N_\Phi} \sum_{\boldsymbol{\phi}\in\Phi^i} \mathcal{F}_2^r(\boldsymbol{\phi})\omega_{k|k}(\boldsymbol{\phi})\delta_k \\ &= \sum_{i=1}^{N_\Phi}\left(\sum_{r=1}^{R} \mathcal{F}_1^r(\boldsymbol{\xi}) \sum_{\boldsymbol{\phi}\in\Phi^i} \mathcal{F}_2^r(\boldsymbol{\phi})\omega_{k|k}(\boldsymbol{\phi})\delta_k\right),\end{aligned} \tag{18}$$

where $\tilde{\omega}_{k+1|k}(\boldsymbol{\xi})$ and $\omega_{k|k}(\boldsymbol{\phi})$ denote the weights corresponding to $\boldsymbol{\xi}$ and $\boldsymbol{\phi}$, respectively. Note that the sums $\sum_{i=1}^{N_\Phi}\sum_{\boldsymbol{\phi}\in\Phi^i} \mathcal{F}_2^r(\boldsymbol{\phi})$ (summing over subgrids Φ^i and the points in each) are equivalent to the sum $\sum_{i=1}^{N} \mathcal{F}_2^r(\boldsymbol{\phi}^{(i)})$ (summing over all points in Φ). Then, for each combination of the subgrids Ξ^j and Φ^j, $j = 1, \ldots, N_\Xi, i = 1, \ldots, N_\Phi$ a single shift vector $\boldsymbol{\zeta}^{i,j}$ is calculated similarly to (17).

The computation of the predictive PDF value (18) can be seen as convolutions proceeding in *two levels*. The *upper-level convolution* combines each subgrid Φ^i, $i = 1, \ldots, N_\Phi$ with all subgrids Ξ^j, $j = 1, \ldots, N_\Xi$ by computing the values $\boldsymbol{\zeta}^{i,j}$ for shifting these subgrids. The *lower-level convolution* employs the functional decomposition (the parenthesis in (18)) by processing the gridpoints of Ξ^j and the gridpoints of Φ^i:

$$\tilde{\omega}_{k+1|k}(\boldsymbol{\xi}) = \sum_{i=1}^{N_\Phi} \left(\sum_{r=1}^{R} \mathcal{F}_1^r(\boldsymbol{\xi} - \boldsymbol{\zeta}^{i,j}) \sum_{\boldsymbol{\phi}\in\Phi^i} \mathcal{F}_2^r(\boldsymbol{\phi} - \boldsymbol{\zeta}^{i,j})\omega_{k|k}(\boldsymbol{\phi})\delta_k\right), \tag{19}$$

where $\boldsymbol{\xi} \in \Xi^j$.

As the construction of Ξ_{k+1} proceeds from Φ_k as $\mathbf{x}_{k+1} = \mathbf{f}_k + \mathbf{w}_k$, the grids usually have significant overlap. This can increase efficiency in the predictive PDF calculation by assessing the closeness of individual subgrids. Here the closeness relates to the covariance matrix of $\mathbf{w}_k$ and associated confidence sets. If the norm $\|\boldsymbol{\xi} - \boldsymbol{\phi}\|_{(\Sigma_k^{\mathbf{w}})^{-1}}$ with $\Sigma_k^{\mathbf{w}} = \mathrm{var}[\mathbf{w}_k]$ is large $\forall \boldsymbol{\xi} \in \Xi^j$ and $\forall \boldsymbol{\phi} \in \Phi^i$, then the value of the transient PDF (15) is close to zero and this combination of subgrids can be omitted from the calculation. Thus, some combinations of subgrids Ξ^j, $j = 1, \ldots, N_\Xi$ and Φ^i, $i = 1, \ldots, N_\Phi$ can be dropped in (19). This approach is similar to the thrifty convolution proposed in (Šimandl et al., 2006) with the difference of proceeding in the upper-level convolution for the whole subgrids.

3.3 Subgrid Size and Complexity

As mentioned, the subgrids of Ξ and Φ should be designed so that they fit (after the shifting) into the approximation region Ω. This ensures that the processing of subgrids Ξ^j and Φ^i by the lower-level convolution (involving the functional decomposition) does not lead to zero prediction PDF caused the limited size of the approximation region. Decreasing the subgrids' size increases their number N_Ξ and N_Φ, respectively, resulting in more shifts and increased computational complexity. As $N_\Xi \to N$ and $N_\Phi \to N$, the complexity of this two-level convolution approaches that of the FC.

In terms of a function evaluation, the FC requires $\mathcal{O}(N^2)$ evaluations of the transient PDF. Using the FTD of the transient PDF requires $\mathcal{O}((2N+1)R)$ evaluations of the function $\mathcal{F}$. Thus, the savings due to the decomposition can be expected for $N \gg R$. Assuming that subgrids $\{\Xi^j\}_{j=1}^{N_\Xi}$ have an equal number of gridpoints N/N_Ξ and subgrids $\{\Phi^j\}_{j=1}^{N_\Phi}$ have an equal number of gridpoints N/N_Φ, then the proposed two-level convolution requires

$$\mathcal{O}\left(N_\Xi N_\Phi\left(\frac{N}{N_\Xi}R + \frac{N}{N_\Phi}R + R\right)\right) = \mathcal{O}((N_\Phi N + N_\Xi N + 1)R) \tag{20}$$

operations. The complexity thus depends on the number of subgrids N_Ξ and N_Φ. Note that when the subgrids have only a single grid point (i.e., $N_\Xi = N$, $N_\Phi = N$), then the number of $\mathcal{F}$ evaluations is $\mathcal{O}((2N^2+1)R)$, which means higher computational complexity than the FC. If, on the other hand, there are only single subgrids (i.e., $N_\Xi = 1$, $N_\Phi = 1$), then the number of $\mathcal{F}$ evaluations is $\mathcal{O}((2N+1)R)$, which means the same computational complexity as the FTD-based convolution proposed by Tichavský et al. (2022). While the complexity (20) of the proposed two-level convolution will always be higher

than the complexity of the original FTD-based convolution for the same rank R, the two-level convolution allows to use a small approximation region Ω, which leads to smaller rank and reduced complexity as a result.

3.4 Algorithm of PMF with two-level convolution

The algorithm of the PMF with the proposed two-level convolution (with full combination of the subgrids) is as follows.

Algorithm 2: Point-Mass Filter with Two-level Convolution

(1) *Initialization*: (same as in Algorithm 1)
(2) *Meas. update*: (same as in Algorithm 1)
(3) *Grid construction:* Construct the new grid Ξ_{k+1} and split it into $N_{\Xi_{k+1}}$ subgrids Ξ^j_{k+1}, $j = 1, \dots, N_{\Xi_{k+1}}$.
(4) *Time update*:
  (a) Propagate the gridpoints $\boldsymbol{\xi}^{(i)}_k$ of Ξ_k through the dynamics function $\mathbf{f}_k(\boldsymbol{\xi}^{(i)}_k, \mathbf{u}_k)$ to obtain the gridpoints $\boldsymbol{\phi}^{(i)}_k$ of Φ_k.
  (b) Split Φ_k into N_{Φ_k} subgrids Φ^i_0, $i = 1, \dots, N_{\Phi_k}$.
  (c) For each pair of subgrids Φ^i_k and Ξ^j_{k+1}, $i = 1, \dots, N_{\Phi_k}$ and $j = 1, \dots, N_{\Xi_k}$ calculate the shift value $\boldsymbol{\zeta}^{i,j}$.
  (d) Compute the predictive point-mass PDF of the form (5) at gridpoints of $\mathbf{X}_{k+1}$ according to (19).
  (e) Normalize the values as $\omega^{(j)}_{k+1|k} = c^{-1}_{k+1}\tilde{\omega}^{(j)}_{k+1|k}$, where $c_{k+1} = \sum_{j=1}^{N}\tilde{\omega}^{(j)}_{k+1|k}$.
(5) Set $k = k + 1$ and go to Step 2.

Note that using the thrifty combination of the subgrids as described in Section 3 would affect step (4d).

3.5 Subgrid Design in Multiple Dimensions

Section 3.2 described the construction of the subgrids for the scalar state, $n_x = 1$, which will now be generalized to case $n_x > 1$. The usual approach to design the grid [8] Ξ is to (I) specify a grid for each axis $\Psi(i) = \{\psi^{(j_i)}(i)\}$, $j_i = 1, \dots N_{\Psi(i)}$ $i = 1, \dots n_x$ (further called *axis grid*) and (II) combine the points of the axis grids as $\boldsymbol{\xi}^{(\ell)} = [\psi^{(j_1)}(1), \psi^{(j_2)}(2), \dots, \psi^{(j_{n_x})}(n_x)]^\top$, $j_i = 1, \dots N_{\Psi(i)}$, $i = 1, \dots n_x$. The number of points of Ξ is then $N = \prod_{i=1}^{n_x} N_{\Psi(i)}$.

Designing a new grid Ξ_{k+1} in step (3) of Algorithm 2 and its subsequent splitting can be conveniently replaced by a straight construction of the subgrids Ξ^j_{k+1}, $j = 1, \dots N_\Xi$. First, each axis grid $\Psi(i)$ is split into $M(i)$ subgrids. Combining these subgrids (one for each dimension) will lead to a subgrid Ξ^ℓ and the total number of these subgrids will be $N_\Xi = \prod_{i=1}^{n_x} M(i)$. The procedure is illustrated in Fig. 3 for $n_x = 2$.

4. NUMERICAL ILLUSTRATION

The performance of the proposed two-layer convolution is illustrated in this section for $n_x = 2$ in terms of computational time and accuracy of the prediction PDF (4) computation. For convenience, the state dynamics was chosen as $\mathbf{f}_k(\mathbf{x}_k, \mathbf{u}_k) = \mathbf{x}_k$. Note that the choice of $\mathbf{f}$ has no effect on the proposed decomposition. For the performance analysis, the process noise

[8] The time index is again dropped here for convenience.

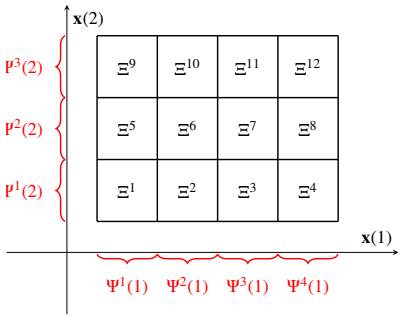

Fig. 3. Illustration of construction of subgrids Ξ^ℓ for $n_x = 2$ from axis subgrids $\Psi^i(1)$ and $\Psi^j(2)$. The symbol $\mathbf{x}(i)$ denotes i-th element of $\mathbf{x}$.

PDF was assumed standard Gaussian [9] $p(\mathbf{w}_k) = \mathcal{N}\{\mathbf{w}_k, \mathbf{0}, \mathbf{I}_{n_x}\}$, where $\mathbf{I}_{n_x}$ is the $n_x \times n_x$ dimensional identity matrix. The grids Φ_k and Ξ_{k+1} were constructed using $N = 100^{n_x} = 10\,000$ points for each grid regularly spread in the region $[-20, 20] \times [-20, 20]$ The weights of the gridpoints Φ_k were equal $\omega_{k|k}(\boldsymbol{\phi}^{(i)}) = \frac{1}{N}$, $\forall i$. Two approximation regions were considered $\Omega' = [-5, 5] \times [-5, 5]$ (see Fig. 2 for illustration) and $\Omega'' = [-10, 10] \times [-10, 10]$ (see Fig. 1 for illustration). The parameters for the functional decomposition were adopted from (Tichavský et al., 2022) for $n_x = 2$ in the form

$$\mathcal{F}^r_1(\mathbf{x}) = \mathcal{F}^r_2(\mathbf{x}) = \beta^{n_x} \cdot e^{-\frac{\|\mathbf{x}-\boldsymbol{\mu}^r\|^2}{2\sigma^2}} = \beta^2 \cdot e^{-\frac{1}{2\sigma^2}\left[(\mathbf{x}(1)-\boldsymbol{\mu}^r(1))^2+(\mathbf{x}(2)-\boldsymbol{\mu}^r(2))^2\right]},$$

with the parameters $\sigma = 0.7088$ and $\beta = 0.1008$ and location parameters $\boldsymbol{\mu}^r$ forming regular orthogonal lattices covering Ω' and Ω'' with distance $d = 1$ between adjacent location parameters. These values were obtained by optimization [10] and led to ranks $R' = 100$ for Ω' and $R'' = 400$ for Ω''. Four approaches [11] calculating the predictive PDF (4) were used:

- Full convolution (FC) given by (9),
- Thrifty convolution (TC) (Šimandl et al., 2002),
- FTD-based convolution (Tichavský et al., 2022) (FTDC) for Ω' and Ω'',
- Two-level convolution (2LC) that split both Ξ_{k+1} and Φ_k into $N_{\Xi_{k+1}} = N_{\Phi_k} = 16$ subgrids of equal size.

The approaches are compared in terms of computational time and relative error, defined as

$$\mathrm{RERR} = 100\frac{\left|p(\mathbf{x}_{k+1}|\mathbf{z}^k) - \hat{p}(\mathbf{x}_{k+1}|\mathbf{z}^k)\right|}{p(\mathbf{x}_{k+1}|\mathbf{z}^k)},$$

where $p(\mathbf{x}_{k+1}|\mathbf{z}^k)$ denotes the PDF calculated by FC and $\hat{p}(\mathbf{x}_{k+1}|\mathbf{z}^k)$ is the PDF calculated by TC, FTDC, or 2LC.

The values of relative error in [%] for TC, FTDC(Ω'), FTDC(Ω''), and 2LC(Ω') are depicted in Figure 4. The computational time and integral of RERR over the state space are given in Table 1.

The results show that the FC is the most computationally demanding approach, while the FTDCs are the cheapest. However, when the relative error is compared, the largest value is achieved by FTDC(Ω') because of too small Ω' in comparison with the

[9] Note that the decomposition can be computed for any noise distributions such as the Student-t, generalized Gaussian, or Cauchy PDF (Tichavský et al., 2023).
[10] For details on the optimization, see (Tichavský et al., 2023).
[11] The Rao-Blackwellization and separable prediction techniques were not included in the comparison as they assume a special form of the transient PDF.

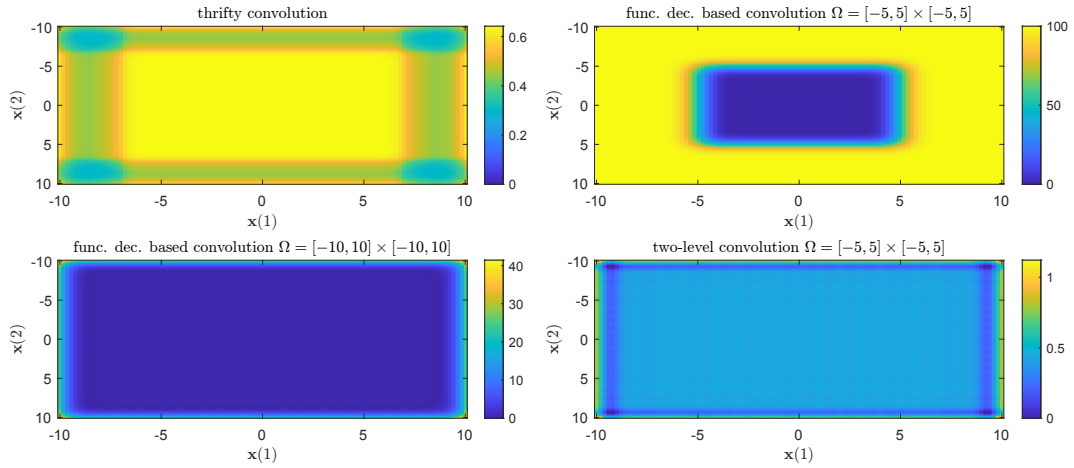

Fig. 4. Relative error in [%] for TC, FTDC, and 2LC.

Table 1. Computational time and integral of RERR (IRERR) for the different calculations of predictive PDF.

	FC	TC	FTDC(Ω')	FTDC(Ω'')	2LC(Ω')
$\oslash T$ [s]	2.23	1.94	0.11	0.32	0.39
IRERR [%]	—	0.54	75.47	2.69	0.43

grids Ξ_{k+1} and Φ_k. Enlarging the approximation region four times reduces the error FTDC(Ω''). However, the proposed 2LC achieves the smallest error even for the small region Ω'. RERR of TC is close to that of 2LC but at the cost of almost five times higher costs. Note that the differences in performance would be more pronounced for higher state dimensions n_x.

5. CONCLUSION

The paper dealt with the prediction step of the point mass filter that involves convolving two grids. The functional decomposition-based convolution was elaborated for the cases when the approximation region is smaller than the grids leading to large errors. The aim was to keep the size of the approximation region and, consequently the rank of the decomposition small to keep computational complexity small. The proposed solution involves splitting the grids into a set of subgrids and convolving the subgrid pairs using functional decomposition. This leads to a two-level convolution that processes the subgrids at the upper level and their gridpoints at the lower level. The numerical example demonstrated a small relative error achieved by the proposed technique while keeping the computational cost low.

REFERENCES

Arasaratnam, I. and Haykin, S. (2009). Cubature Kalman filters. *IEEE Trans. on Automatic Control*, 54(6), 1254–1269.

Bergman, N. (1999). *Recursive Bayesian Estimation: Navigation and Tracking Applications*. Ph.D. thesis, Linköping University, Sweden.

Chen, J.C. (1984). The nonnegative rank factorizations of nonnegative matrices. *Linear Algebra and its Applications*, 62, 207–217.

Doucet, A., De Freitas, N., and Gordon, N. (eds.) (2001). *Sequential Monte Carlo Methods in Practice*. Springer. (Ed. Doucet A., de Freitas N., and Gordon N.).

Duník, J., Soták, M., Veselý, M., Straka, O., and Hawkinson, W.J. (2019). Design of Rao-Blackwellised point-mass filter with application in terrain aided navigation. *IEEE Trans. on Aerospace and Electronic Systems*, 55(1), 251–272.

Duník, J., Straka, O., Matoušek, J., and Blasch, E. (2022). Copula-based convolution for fast point-mass prediction. *Signal Processing*, 192(), 108367.

Gorodetsky, A.A., Karaman, S., and Marzouk, Y.M. (2018). A continuous analogue of the tensor-train decomposition. arXiv:1510.09088 [math.NA].

Huang, K., Sidiropoulos, N.D., and Swami, A. (2014). Non-negative matrix factorization revisited: Uniqueness and algorithm for symmetric decomposition. *IEEE Trans. on Signal Processing*, 62(1), 211–224.

Kalender, C. and Schottl, A. (2013). Sparse grid-based nonlinear filtering. *IEEE Transactions on Aerospace and Electronic Systems*, 49(4), 2386–2396.

Lim, J.N. and Park, C.G. (2019). RBPPFF for robust TAN. *IET Radar, Sonar and Navigation*, 13(12), 2230–2243.

Matoušek, J., Duník, J., and Straka, O. (2019). Point-mass filter: Density specific grid design and implementation. In *Proceedings of the 15th European Workshop on Advanced Control and Diagnosis*. Bologna, Italy.

Nelsen, R.B. (2006). *An Introduction to Copulas*. Springer, New York, NY, USA, second edition.

Paatero, P. and Tapper, U. (1994). Positive matrix factorization: A non-negative factor model with optimal utilization of error estimates of data values. *Environmetrics*, 5(2), 111–126.

Särkkä, S. (2013). *Bayesian Filtering and Smoothing*. Cambridge University Press.

Sorenson, H.W. and Alspach, D.L. (1971). Recursive Bayesian estimation using Gaussian sums. *Automatica*, 7, 465–479.

Tichavský, P., Straka, O., and Duník, J. (2022). Point-mass filter with decomposition of transient density. In *Proceedings of the 2022 IEEE International Conference on Acoustics, Speech and Signal Processing (ICASSP)*, 5752–5756.

Tichavský, P., Straka, O., and Duník, J. (2023). Grid-based bayesian filters with functional decomposition of transient density. *IEEE Trans. on Signal Processing*, 71, 92–104.

Šimandl, M., Královec, J., and Söderström, T. (2002). Anticipative grid design in point-mass approach to nonlinear state estimation. *IEEE Trans. on Automatic Control*, 47(4).

Šimandl, M., Královec, J., and Söderström, T. (2006). Advanced point-mass method for nonlinear state estimation. *Automatica*, 42(7), 1133–1145.